# Distributed Model Predictive Load Frequency Control of Multi-area Power System with DFIGs

Yi Zhang, Xiangjie Liu, and Bin Qu

*Abstract*—Reliable load frequency control (LFC) is crucial to the operation and design of modern electric power systems. Considering the LFC problem of a four-area interconnected power system with wind turbines, this paper presents a distributed model predictive control (DMPC) based on coordination scheme. The proposed algorithm solves a series of local optimization problems to minimize a performance objective for each control area. The generation rate constraints (GRCs), load disturbance changes, and the wind speed constraints are considered. Furthermore, the DMPC algorithm may reduce the impact of the randomness and intermittence of wind turbine effectively. A performance comparison between the proposed controller with and without the participation of the wind turbines is carried out. Analysis and simulation results show possible improvements on closed–loop performance, and computational burden with the physical constraints.

*Index Terms*—Distributed model predictive control (DMPC), doubly fed induction generator (DFIG), load frequency control (LFC).

## I. INTRODUCTION

LOAD frequency control (LFC) and secondary frequency control, have been performed integrating the area control error (ACE), which acts on the load reference settings of the governors. LFC tasks are maintaining tie-line power flow and system frequency close to nominal value for the multi-area interconnected power system [1]. Generation in modern electric power systems comprises of mix type of thermal, hydro, nuclear, gas power generation and even wind generation. Presently, the thermal and hydro units are the major choice of LFC. The advanced modeling and control strategies utilized

in LFC problem can be found in several recent overviews [2], [3].

Wind energy has recently been the major renewable energy sources, due to its socioeconomic and environmental benefits. The world market of wind installation set a new record in the year of 2014 and reached a total size of 51 GW [4]. Due to the increasing portion of wind turbine generations (WTGs) within the whole power system, it will inevitably participate in LFC. In most power systems, the output power of wind turbine generators varies with wind speed fluctuation, this fluctuation results into frequency variation. Previous studies [5]−[7] provide extensive overviews of the primary and secondary frequency control strategies for power systems with wind power plants.

Due to the randomness and intermittence of the wind power, the controllability and availability of wind power significantly differs from conventional power generation. It is necessary to reconstruct the LFC structure incorporating the dynamic model of WTGs, in which every output power of the WTGs is monitored and checked with individual reference command.

Recently, a few attempts studied the idea of wind turbines with the issue of LFC [8]−[10]. Two types of wind farm models are derived and demonstrated to portray the capability of set-point tracking under automatic generation control (AGC) [8]. An adaptive fuzzy logic structure was used to propose a new LFC scheme in the interconnected large-scale power system in the presence of wind turbines [9]. The performance against sudden load change and wind power fluctuations in different wind power penetration rates are confirmed by simulation. A flatness-based method to control frequency and power flow for multi-area power system with wind turbine is presented in [10]. And, practical constraints such as generator ramping rates of wind turbine generator are considered in designing the controllers. As above-mentioned reference, the control schemes are designed for each area to maintain the frequency at nominal value and to keep power flows near scheduled values. However, local controller in each area does not work cooperatively towards satisfying system-wide control objectives. In addition, the control schemes [8]−[10] mentioned above could yield unsatisfactory performance since the effects of nonlinearities such as Generation Rate Constraint is not considered.

Model predictive control (MPC), also called receding horizon control, was originally developed to be an effective method for processing industrial control. In the power industry, MPC has been successfully used in controlling power plant steam-boiler generation processes [11]−[13]. MPC has subsequently been developed to realize the constrained optimal algorithm

Y. Zhang is with the Department of Electrical Engineering, North China University of Science and Technology, Tangshan 063000, China, and also with the State Key Laboratory of Alternate Electrical Power System with Renewable Energy Sources, North China Electric Power University, Beijing 102206, China (e-mail: zhangyizhouzhao@163.com).

X. J. Liu is with the State Key Laboratory of Alternate Electrical Power System with Renewable Energy Sources, North China Electric Power University, Beijing 102206, China (e-mail: liuxj@ncepu.edu.cn).

B. Qu is with the Department of Electrical Engineering, North China University of Science and Technology, Tangshan 063000, China (e-mail: qubin@ncst.edu.cn).

for an LFC problem. The centralized model of power system is used for predicting the state variables. Then, centralized MPC transforms the control problem into a global optimization problem that can satisfy multivariable constraints on the generation rate constraints (GRCs) and input constraints. In [14], the constraint handling ability of MPC is employed to effectively account for the generation rate constraints. Recently, MPC has been successfully used in an LFC design of multi-area power system with wind turbines [15]. However, with the size and capacity of wind farms which have increased in recent years traditional centralized MPC encounters many difficulties due to limitations in exchanging information with large-scale, geographically expansive control areas. In order to deal with these issues, advanced distributed control strategies have to be investigated and implemented.

Developing decentralized/distributed LFC structures can be an effective way of solving the above mentioned problems. In the decentralized LFC framework, the overall power system is decomposed into several subsystems and each has its own local area MPC controller. These local MPC controllers optimize local control objective function and the interaction between the control areas is negligible. The decentralized model predictive control scheme for the LFC of multi-area interconnected power system is presented in [16]. However, the local controller does not consider generation rate constraint that is only imposed on the turbine in the simulation. In the DMPC, the benefits from using a decentralized structure are partially preserved, and the performance and stability are improved through coordination [17], [18]. In [19], feasible cooperation-based MPC method is used in distributed LFC instead of centralized MPC. It is noted that the range of load change used in the cases is very large and inappropriate for the LFC issue.

This paper aims to design the distributed model predictive controller for the LFC of the multi-area power system with DFIGs. The main contributions of this work can be summarized as follows: 1) The structure of wind turbine participated in the LFC as the complement of the thermal plants or hydro plants is established. The distributed model for power system is derived from the above LFC structure. 2) The distributed MPC controllers in each area exchange their measurements and predictions by communication and incorporate the information from other controllers into their local control objective so as to coordinate with each other. 3) The GRCs, load setpoint constraint and wind speed constraints are considered as state and input constraints in the DMPC.

The remainder of the paper is organized as follows. Modeling of wind turbines participation in LFC is presented in Section II, and the proposed DMPC algorithm is presented in Section III. Section IV presents the application of the algorithm in a four-area interconnected power system. The conclusions are presented in Section V.

## II. DISTRIBUTED MODEL OF HYBRID POWER SYSTEM

A large-scale multi-area interconnected power system comprises of several control areas, connected by tie-lines. A load change in any area can cause a transient frequency change in all control areas. The generation within each area has to be controlled so as to maintain scheduled power interchange. The

LFC system should control the inter-change power of the local control area with the other control areas as well as its local frequency.

Generation in modern power systems comprises of mix type of thermal, hydro, nuclear, gas power generation and even wind generation. In China, the total generation capacity of thermal and hydro power generation has reached $916\,\mathrm{GW}$ and $302\,\mathrm{GW}$ until the year 2014, representing $67.4\,\%$ and $22.2\,\%$ respectively. At present, the major choice of automatic generation control (AGC) falls on thermal unit. Therefore, the block of four-area power system is illustrated in Fig. 1, where the thermal power plant and wind farm are in Area 1, and the power plants in Areas 2, 3 and 4 are just thermal power plants.
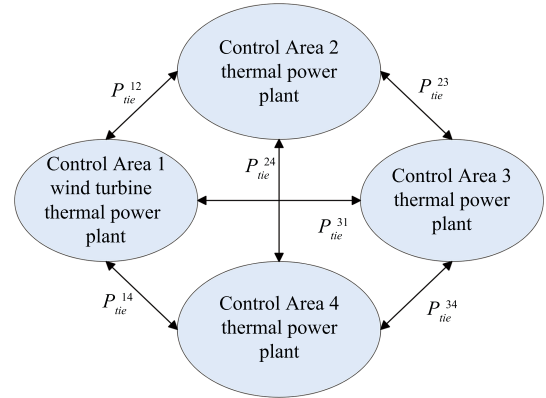


Fig. 1.   The four-area interconnected hybrid power system.

Detailed compositions of each power plant are shown in Figs. 2−3 [14]. In addition, Area 1 includes an aggregated wind turbine model which consists of 50 wind turbine units of 2 MW rated DFIG. The variables and parameters of model are listed in Table I. In each control area, a change in local demand (load) alters the nominal frequency. The DMPC in each control area $i$ manipulates the control variable to drive the frequency deviations $\Delta f_i$ and tie-line power flow deviations $\Delta P_{tie,ij}$ to zero.

### A. Wind Turbine Model

A simplified model of DFIG is shown in [20]. This simplified model can be described by the following equations:

$$\dot{i}_{qr} = -\left(\frac{1}{T_1}\right)i_{qr} + \left(\frac{X_2}{T_1}\right)V_{qr} \tag{1}$$

$$\dot{w}_r = -\left(\frac{X_3}{2H_t}\right)i_{qr} + \left(\frac{1}{2H_t}\right)T_m \tag{2}$$

$$P_e = w_{opt}X_3 i_{qr} \tag{3}$$

$$T_e = i_{qs} = -\frac{L_m}{L_{ss}}i_{qr} \tag{4}$$

where $X_2 = 1/R_r$, $X_3 = L_m/L_{ss}$, $T_1 = L_0/w_{ss}R_s$, $L_{33} = L_s + L_m$, $L_0 = [L_{rr} + L_m^2/L_{ss}]$, $L_{rr} = L_r + L_m$, and $L_m$ is the magnetizing inductance, $R_r$ and $R_s$ are the rotor and stator resistances, respectively. $L_r$ and $L_s$ are the rotor and stator leakage inductances, respectively. $L_{rr}$ and $L_{ss}$ are the rotor and stator self-inductances, respectively.
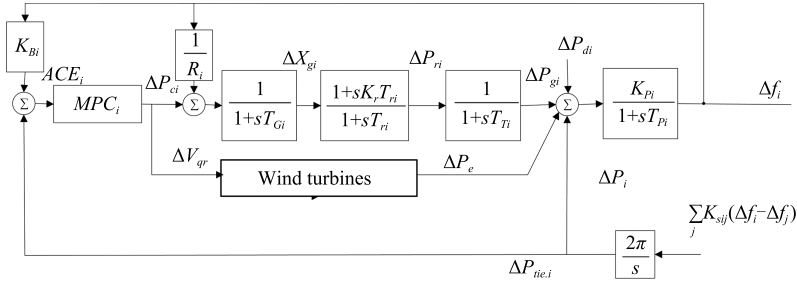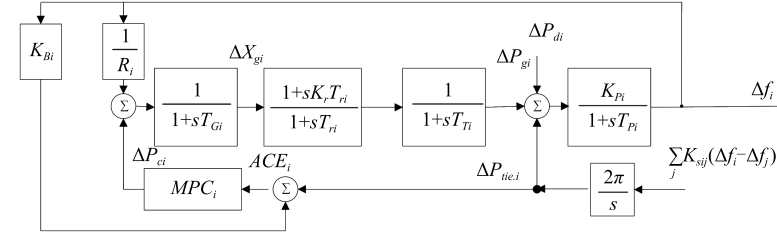
Fig. 2. Block diagram of a thermal power plant and wind power plant ($i = 1$).



Fig. 3. Block diagram of a thermal power plant ($i = 2, 3, 4$).

TABLE I
POWER SYSTEM VARIABLES AND PARAMETER

| Parameter/ Variable | Description | Unit |
|---|---|---|
| $w_{opt}$ | Operating point of the rotational speed | rad/s |
| $w_s$ | Synchronous speed | rad/s |
| $i_{qr}$ | $q$-axis component of the rotor current | |
| $V_{qr}$ | $q$-axis component of the rotor voltage | |
| $T_e$ | Electromagnetic torque | Nm |
| $T_m$ | Mechanical power torque | Nm |
| $H_t$ | Equivalent inertia constant of wind turbine | |
| $P_e^{ref}$ | Power demand | p.u.MW |
| $P_e$ | The output of wind turbine | p.u.MW |
| $\Delta f_i(t)$ | Frequency deviation | Hz |
| $\Delta P_{gi}(t)$ | Generator output power deviation | p.u.MW |
| $\Delta X_{gi}(t)$ | Governor valve position deviation | p.u. |
| $\Delta X_{ghi}(t)$ | Governor valve servomotor position deviation | p.u. |
| $\Delta P_{tie,i}(t)$ | Tie-line active power deviation | p.u.MW |
| $\Delta P_{di}(t)$ | Load disturbance | p.u.MW |
| $K_{Pi}$ | Power system gain | Hz/p.u.MW |
| $K_{ri}$ | Reheat turbine gain | Hz/p.u.MW |
| $T_{Pi}$ | Power system time constant | s |
| $T_{ri}$ | Reheat turbine time constant | s |
| $T_{Gi}$ | Thermal governor time constant | s |
| $T_{Ti}$ | Turbine time constant | s |
| $K_{Sij}$ | Interconnection gain between control areas | p.u.MW |
| $K_{Bi}$ | Frequency bias factor | p.u.MW/Hz |
| $R_i$ | Speed drop due to governor action | Hz/p.u.MW |
| $ACE_i$ | Area control error | p.u.MW |

## B. Model of Thermal Power Plant

Consider control area $i$, $i \in 1, \ldots, 4$, to be interconnected with the control area $j$ through a tie-line. A simplified model for any thermal power plant in each area is described in [14]. The overall generator load dynamic relationship between the incremental mismatch power ($\Delta P_{gi} - \Delta P_{di}$) and the frequency deviation $\Delta f_i$ can be expressed as

$$\Delta \dot{f}_i = -\frac{1}{T_{pi}}\Delta f_i - \frac{K_{pi}}{T_{pi}}\Delta P_{tie,i} + \frac{K_{pi}}{T_{pi}}\Delta P_{gi}$$
$$- \frac{K_{pi}}{T_{pi}}\Delta P_{di} + \frac{1}{T_{Gi}}\Delta P_{ci}. \tag{5}$$

The dynamics of the turbine can be expressed as

$$\Delta \dot{P}_{gi} = -\frac{1}{T_{Ti}}\Delta P_{gi} - \frac{1}{T_{Ti}}\Delta P_{ri}. \tag{6}$$

The dynamic equation of the governor can be expressed as

$$\Delta \dot{X}_{gi} = -\frac{1}{T_{Gi}R_i}\Delta f_i - \frac{1}{T_{Gi}}\Delta X_{gi}. \tag{7}$$

The dynamic equation of the reheat component of the turbine can be expressed as

$$\Delta \dot{P}_{ri} = -\frac{K_{ri}}{T_{Gi}R_i}\Delta f_i + \left(\frac{1}{T_{ri}} - \frac{K_{ri}}{T_{Gi}}\right)\Delta X_{gi} - \frac{1}{T_{ri}}\Delta P_{ri}. \tag{8}$$

The tie-line power flow between areas $i$ and $j$ can be described as

$$\Delta \dot{P}_{tie}^{ij} = K_{sij}\left(\Delta f_i - \Delta f_j\right), \quad \Delta P_{tie}^{ij} = -\Delta P_{tie}^{ji}. \tag{9}$$

The total tie-line power change between areas $i$ and $j$ and other areas can be computed by

$$\Delta \dot{P}_{tie,i} = \sum_{\substack{j=1 \\ j \neq i}}^{4} \Delta \dot{P}_{tie}^{ij} = \sum_{\substack{j=1 \\ j \neq i}}^{4} K_{sij}\left(\Delta f_i - \Delta f_j\right). \tag{10}$$

In a multi-area power system, in addition to regulating area frequency, the interchange power with neighboring area should be maintained at scheduled value. Area control error (ACE) indicates the power mismatch between the area load and generation. The $ACE_i$ for control area $i$ can be expressed

as a summation of frequency deviation $\Delta f_i$ multiplied by a bias factor $K_{Bi}$ and tie-line power change $\Delta P_{tie,i}$:

$$ACE_i = [K_{Bi}\Delta f_i + \Delta P_{tie,i}]. \qquad (11)$$

### C. Model of Four-area Power System With Wind Turbine

In this section, the state space model will be established for the four-area power system. The above DFIG model (1)−(2) and thermal plant model (6)−(11) for Area 1 of power system control area can be combined in the following state space model:

$$
\begin{bmatrix}
\Delta \dot{f}_i \\
\Delta \dot{P}_{tie,i} \\
\Delta \dot{P}_{gi} \\
\Delta \dot{X}_{Gi} \\
\Delta \dot{P}_{ri} \\
\Delta \dot{i}_{qr} \\
\Delta \dot{w}_i
\end{bmatrix} =
$$

$$
\begin{bmatrix}
-\frac{1}{T_{Pi}} & -\frac{K_{Pi}}{T_{Pi}} & \frac{K_{Pi}}{T_{Pi}} & 0 & 0 & 0 & 0 \\
\sum_j K_{sij} & 0 & 0 & 0 & 0 & 0 & 0 \\
0 & 0 & -\frac{1}{T_{Ti}} & 0 & \frac{1}{T_{Ti}} & 0 & 0 \\
-\frac{1}{T_{Gi}R_i} & 0 & 0 & -\frac{1}{T_{Gi}} & 0 & 0 & 0 \\
-\frac{K_{ri}}{T_{Gi}R_i} & 0 & 0 & \frac{1}{T_{ri}}-\frac{K_{ri}}{T_{Gi}} & \frac{1}{T_{ri}} & 0 & 0 \\
0 & 0 & 0 & 0 & 0 & -\frac{1}{T_1} & 0 \\
0 & 0 & 0 & 0 & 0 & -\frac{X_3}{2H_t} & 0
\end{bmatrix}
$$

$$
\times
\begin{bmatrix}
\Delta f_i \\
\Delta P_{tie,i} \\
\Delta P_{gi} \\
\Delta X_{Gi} \\
\Delta P_{ri} \\
\Delta i_{qr} \\
\Delta w_i
\end{bmatrix} +
\begin{bmatrix}
\frac{1}{T_{Gi}} & 0 \\
0 & 0 \\
0 & 0 \\
0 & 0 \\
0 & 0 \\
0 & \frac{X_2}{T_1} \\
0 & 0
\end{bmatrix}
\begin{bmatrix}
\Delta P_{ci} \\
\Delta V_{qr}
\end{bmatrix} +
\begin{bmatrix}
-\frac{K_{Pi}}{T_{Pi}} & 0 \\
0 & 0 \\
0 & 0 \\
0 & 0 \\
0 & 0 \\
0 & 0 \\
0 & 1
\end{bmatrix}
\begin{bmatrix}
\Delta P_{di} \\
\Delta v_m
\end{bmatrix}
$$

$$(12)$$

$$
y_i = ACE_i = \begin{bmatrix} K_{Bi} & 1 & 0 & 0 & 0 & 0 & 0 \end{bmatrix}
$$
$$
\begin{bmatrix} \Delta f_i & \Delta P_{tie,i} & \Delta P_{gi} & \Delta X_{Gi} & \Delta P_{ri} & \Delta i_{qr} & \Delta w_i \end{bmatrix}^T. \qquad (13)
$$

The state space model of thermal power plant in area $i$ ($i = 2, 3, 4$) can be expressed as

$$
\begin{bmatrix}
\Delta \dot{f}_i \\
\Delta \dot{P}_{tie,i} \\
\Delta \dot{P}_{gi} \\
\Delta \dot{X}_{Gi} \\
\Delta \dot{P}_{ri}
\end{bmatrix} =
\begin{bmatrix}
-\frac{1}{T_{Pi}} & -\frac{K_{Pi}}{T_{Pi}} & \frac{K_{Pi}}{T_{Pi}} & 0 & 0 \\
\sum_j K_{sij} & 0 & 0 & 0 & 0 \\
0 & 0 & -\frac{1}{T_{Ti}} & 0 & \frac{1}{T_{Ti}} \\
-\frac{1}{T_{Gi}R_i} & 0 & 0 & -\frac{1}{T_{Gi}} & 0 \\
-\frac{K_{ri}}{T_{Gi}R_i} & 0 & 0 & \frac{1}{T_{ri}}-\frac{K_{ri}}{T_{Gi}} & \frac{1}{T_{ri}}
\end{bmatrix}
$$

$$
\times
\begin{bmatrix}
\Delta f_i \\
\Delta P_{tie,i} \\
\Delta P_{gi} \\
\Delta X_{Gi} \\
\Delta P_{ri}
\end{bmatrix} +
\begin{bmatrix}
\frac{1}{T_{Gi}} \\
0 \\
0 \\
0 \\
0
\end{bmatrix}
\Delta P_{ci} +
\begin{bmatrix}
-\frac{K_{Pi}}{T_{Pi}} \\
0 \\
0 \\
0 \\
0
\end{bmatrix}
\Delta P_{di}
$$

$$(14)$$

$$
y_i = ACE_i = \begin{bmatrix} K_{Bi} & 1 & 0 & 0 & 0 \end{bmatrix}
$$
$$
\begin{bmatrix} \Delta f_i & \Delta P_{tie,i} & \Delta P_{gi} & \Delta X_{Gi} & \Delta P_{ri} \end{bmatrix}^T. \qquad (15)
$$

Denoting that the control area to be interconnected with the control area $j$, $j \neq i$ through a tie-line, a linearized time-varying model of control area $i$ can be written as

$$
\begin{cases}
x_i(t) = A_i x_i(t) + B_i u_i(t) + F_i d_i(t) \\
\qquad + \sum_{i \neq j} (A_{ij} x_j(t) + B_{ij} u_j(t)) \\
y_i(t) = C_i x_i(t)
\end{cases} \qquad (16)
$$

where $x_i \in \mathbb{R}^n$, $u_i \in \mathbb{R}^m$, $d_i \in \mathbb{R}^k$, $y_i \in \mathbb{R}^l$ are the state vector, the control signal vector, the disturbance vector and the vector of output of control area $i$, respectively. $x_j \in \mathbb{R}^p u_j \in \mathbb{R}^q$, $d_j \in \mathbb{R}^s$ is the state vector, the control signal vector and the disturbance vector of neighbor control area, respectively. Matrices $A_i$, $B_i$, $C_i$ and $F_i$ represent appropriate system matrices of the control area $i$, $A_{ij}$, $B_{ij}$ and $F_{ij}$ represent the matrices of interaction variables between area $i$ and area $j$.

The state, disturbance and output vectors for area $i$ are defined by

$$
x_1 = \begin{bmatrix} \Delta f_i & \Delta P_{tie,i} & \Delta P_{gi} & \Delta X_{Gi} & \Delta P_{ri} & \Delta i_{qr} & \Delta w_i \end{bmatrix}^T
$$
$$
x_i = \begin{bmatrix} \Delta f_i & \Delta P_{tie,i} & \Delta P_{gi} & \Delta X_{gi} & \Delta P_{ri}(t) \end{bmatrix}^T, \; i = 2, 3, 4
$$
$$
d_1 = \begin{bmatrix} \Delta P_{d1} & \Delta v_m \end{bmatrix}, \quad d_i = \Delta P_{di}, \; i = 2, 3, 4
$$
$$
y_i = ACE_i = [K_{Bi}\Delta f_i + \Delta P_{tie,i}], \; i = 1, 2, 3, 4
$$
$$
u_1 = \begin{bmatrix} \Delta P_{c1} & \Delta V_{qr} \end{bmatrix}^T, u_i = \Delta P_{ci}, \; i = 2, 3, 4.
$$

The state, control and disturbance matrices for Area 1 are

$$
A_1 =
\begin{bmatrix}
-\frac{1}{T_{Pi}} & -\frac{K_{Pi}}{T_{Pi}} & \frac{K_{Pi}}{T_{Pi}} & 0 & 0 & 0 & 0 \\
\sum_j K_{sij} & 0 & 0 & 0 & 0 & 0 & 0 \\
0 & 0 & -\frac{1}{T_{Ti}} & 0 & \frac{1}{T_{Ti}} & 0 & 0 \\
-\frac{1}{T_{Gi}R_i} & 0 & 0 & -\frac{1}{T_{Gi}} & 0 & 0 & 0 \\
-\frac{K_{ri}}{T_{Gi}R_i} & 0 & 0 & \frac{1}{T_{ri}}-\frac{K_{ri}}{T_{Gi}} & \frac{1}{T_{ri}} & 0 & 0 \\
0 & 0 & 0 & 0 & 0 & -\frac{1}{T_1} & 0 \\
0 & 0 & 0 & 0 & 0 & -\frac{X_3}{2H_t} & 0
\end{bmatrix}
$$

$$
B_1 =
\begin{bmatrix}
\frac{1}{T_{Gi}} & 0 & 0 & 0 & 0 & 0 & 0 \\
0 & 0 & 0 & 0 & 0 & \frac{X_2}{T_1} & 0
\end{bmatrix}^T
$$

$$
F_1 =
\begin{bmatrix}
-\frac{K_{Pi}}{T_{Pi}} & 0 & 0 & 0 & 0 & 0 & 0 \\
0 & 0 & 0 & 0 & 0 & 0 & 1
\end{bmatrix}^T
$$

$$
C_1 = \begin{bmatrix} K_{Bi} & 1 & 0 & 0 & 0 & 0 & 0 \end{bmatrix}
$$

while for thermal power plants in Areas 2, 3 and 4 are

$$
A_i =
\begin{bmatrix}
-\frac{1}{T_{Pi}} & -\frac{K_{Pi}}{T_{Pi}} & \frac{K_{Pi}}{T_{Pi}} & 0 & 0 \\
\sum_j K_{Sij} & 0 & 0 & 0 & 0 \\
0 & 0 & -\frac{1}{T_{Ti}} & 0 & \frac{1}{T_{Ti}} \\
-\frac{1}{T_{Gi}R_i} & 0 & 0 & -\frac{1}{T_{Gi}} & 0 \\
-\frac{K_{ri}}{T_{Gi}R_i} & 0 & 0 & \frac{1}{T_{ri}}-\frac{K_{ri}}{T_{Gi}} & -\frac{1}{T_{ri}}
\end{bmatrix}
$$

$$
B_i = \begin{bmatrix} 0 & 0 & 0 & \frac{1}{T_{Gi}} & 0 \end{bmatrix}^T
$$

$$
F_i = \begin{bmatrix} -\frac{K_{pi}}{T_{pi}} & 0 & 0 & 0 & 0 \end{bmatrix}^T
$$

$$
C_i = \begin{bmatrix} K_{Bi} & 1 & 0 & 0 & 0 \end{bmatrix}.
$$

The interaction matrices between the four control areas are

$$A_{ij} = \begin{bmatrix} 0 & 0 & 0 & 0 & 0 & 0 & 0 \\ -K_{Sij} & 0 & 0 & 0 & 0 & 0 & 0 \\ 0 & 0 & 0 & 0 & 0 & 0 & 0 \\ 0 & 0 & 0 & 0 & 0 & 0 & 0 \\ 0 & 0 & 0 & 0 & 0 & 0 & 0 \end{bmatrix}, \quad i = 1; \; j = 2, 3, 4$$

$$A_{ij} = \begin{bmatrix} 0 & -K_{Sij} & 0 & 0 & 0 \\ 0 & 0 & 0 & 0 & 0 \\ 0 & 0 & 0 & 0 & 0 \\ 0 & 0 & 0 & 0 & 0 \end{bmatrix}, \quad i = j = 2, 3, 4; \; i \neq j$$

$$B_{ij} = 0_{7 \times 2}, \quad F_{ij} = 0_{7 \times 2}, \quad i = 1; \; j = 2, 3, 4$$
$$B_{ij} = 0_{5 \times 1}, \quad F_{ij} = 0_{5 \times 1}, \quad i = j = 2, 3, 4.$$

The generation rate constraints (GRC) for all areas are taken into account by adding the limiters to the turbines. The GRC for the thermal plants are $|\Delta \dot{P}_{gi}| \leq 0.0017 \, \text{p.u.MW/s}$. In addition, the load disturbance is constrained to $|\Delta \dot{P}_{d_i}| \leq 0.3$. The wind speed is constrained to $3 \leq v_m \leq 25$.

## III. DISTRIBUTED MODEL PREDICTIVE CONTROLLER

### A. Distributed Model Predictive Controller

The block diagram of the DMPC scheme for a four-area interconnected power system is illustrated in Fig. 4. Though there exist large amount of variables in the interconnected power system, the 30 state variables expressed in equation (12) concerning the frequency, the generator output power, the governor valve(servomotor) position, the tie-line active power the wind speed, $q$-axis component of the rotor voltage and the 4 load disturbance $\Delta P_{di}$ are crucial to LFC problem. They can be measured or estimated directly by the local controller. The DMPC in each area exchanges control information through the power line communication, which is a sole networking technology with high reliability that can provide high speed communication to power grids applications [21].
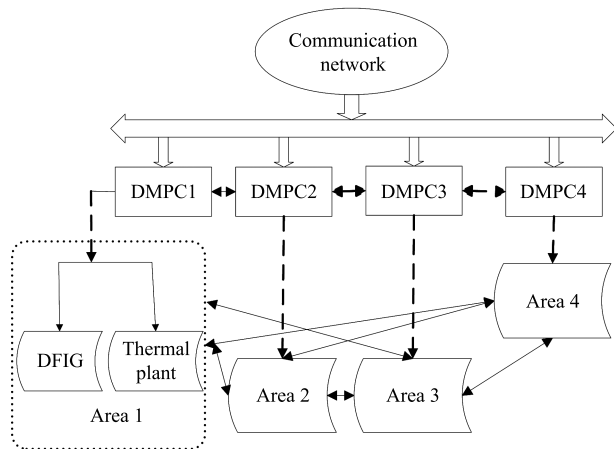


Fig. 4. Block diagram of DMPC for power system.

Generally in the DMPC concept, the discrete-time model for subsystem $i$ of the continuous-time four-area interconnected power system (12) can be expressed as:

$$\bar{x}_i(k+1) = \overline{A}_i \bar{x}_i(k) + \overline{B}_i \bar{u}_i(k) + \overline{F}_i \bar{d}_i(k)$$
$$+ \sum_{j \neq i} (\overline{A}_{ij} \bar{x}_j(k) + \overline{B}_{ij} \bar{u}_j(k))$$
$$\bar{y}_i(k) = \overline{C}_i \bar{x}_i(k). \tag{17}$$

For control area $i = 1$, the cost function of the DMPC design takes into account both the tracking performance of the thermal power plant and the minimization of the wind turbine disturbance to the power system. During the wind farm operation, it is assumed that the mean wind speed of a certain period can be estimated and an initial distribution of individual wind turbine power reference for this period is known. Let $N_c$ denote the control horizon and $N_p$ denote the prediction horizon.

The aims of conventional power plants and DFIG in Area 1 are to regulate the power output according to the load change, expressed as:

$$J_i(k) = \sum_{n=1}^{N_p} \left\{ \|\bar{y}_i(k+n|k) - y_{pref}(k+n|k)\|_{Q_i}^2 \right.$$
$$\left. + \|[\Delta \bar{u}_i(k+n-1|k)]\|_{R_i}^2 \right\}. \tag{18}$$

The optimal problem at instant $k$ can be formulated as follows:

$$\min_{u_i(k+n|k)} J_i(k) \tag{19}$$

s.t.

$$\bar{x}_i(k+1) = \overline{A}_i \bar{x}_i(k) + \overline{B}_i \bar{u}_i(k) + \overline{F}_i d_i(k)$$
$$+ \sum_{j \neq i} (\overline{A}_{ij} \bar{x}_j(k) + \bar{B}_{ij} \bar{u}_j(k))$$
$$3 \leq w_{i2}(k+n|k) \leq 25 \tag{20a}$$
$$|w_{i1}(k+n|k)| \leq 0.3 \tag{20b}$$
$$|x_{i3}(k+n|k)| \leq 0.0017 \tag{20c}$$

where (20a) is the wind speed constraint; (20b) is the load disturbance which is shown as input constraint in each area. (20c) is GRCs of the thermal power plants in Area 1.

For control area $i = 2, 3, 4$, the conventional power plants regulate the output to guarantee load balance of the whole power system and achieve the maximum economical profit simultaneously. The cost function of conventional power plant is expressed as:

$$J_i(k) = \sum_{n=0}^{N_P} [\bar{x}_i^T(k+n|k) Q_i \bar{x}_i(k+n|k)$$
$$+ \bar{u}_i^T(k+n|k) R_i \bar{u}_i(k+n|k)]. \tag{21}$$

The optimal control problem at instant $k$ is formulated as

$$\min_{u_i(k+n|k)} J_i(k) \tag{22}$$

s.t.

$$\bar{x}_i(k+1) = \overline{A}_i \bar{x}_i(k) + \overline{B}_i \bar{u}_i(k) + \overline{F}_i d_i(k)$$
$$+ \sum_{j \neq i} (\overline{A}_{ij} \bar{x}_j(k) + \bar{B}_{ij} \bar{u}_j(k))$$
$$|x_{i3}(k+n|k)| \leq 0.0017 \leq 25 \tag{23a}$$

$$|w_i(k+n|k)| \le 0.3, \quad i = 1,2,3,4 \tag{23b}$$

where (23a) is the GRCs of the thermal power plant in Areas 2, 3, 4, (23b) is the load disturbance which is shown as input constraint in each area.

In the above optimization problem, $Q_i$ and $R_i$ denote positive definite and symmetric weighting matrices. They are tuning parameters to achieve the desired performance and can be chosen freely. The weighting matrices $Q_i$ and $R_i$ in the objective function (18), (21) are chosen as $R_1 = R_2 = R_3 = R_4 = 1$:

$$Q_1 = Q_2 = Q_3 = Q_4 = \mathrm{diag}\,\{1000, 0, 0, 1000\}.$$

Then, by (13), each controller predicts the future state at time $k-1$ and broadcasts it in communication network together with the optimal control sequence over the control horizon. At time $k$, based on the information from the communication network, the optimization problem (15) and (19) is solved in each controller. The DMPC algorithm can be summarized as follow:

*Step 1 (Communication):* The controller in each subsystem $i$ exchanges its previous predictive variables $\bar{x}_i(k)$, $\bar{x}_j(k)$.

*Step 2 (Initialization):* Given the constant matrices $Q_i$, $Q_j$, at instant $k$, given the measured $d_i(k)$.

*Step 3 (Optimization):* $u_i(k)$ is solved by the optimal problem (18) and (21).

*Step 4 (Assignment and prediction):* If the optimal control problem (18) and (21) is feasible, apply to $u_i(k) = \bar{u}_i(k)$, otherwise, $u_i(k) = \bar{u}_i(k-1)$.

*Step 5 (Prediction):* Predict the future states.

*Step 6 (Implementation):* Set $k = k+1$, and return to Step 1 at next sampling time.

*Remark 1:* The proposed DMPC algorithm without stability constraints does not guarantee closed loop stability theoretically. Recently, a variety of different strategies have been proposed to achieve the closed loop system stability in [22], [23]. It requires the transmission of trajectories as opposed to just current state information at each update, which increases the computation and communication requirements. Our future work is focused on pursing the implementation of DMPC with guaranteeing stability and feasibility while reducing the computation and communication requirements.

## IV. SIMULATION RESULTS

In this section, the four-area power system stability is analyzed, the performances of the proposed DMPC have been tested in case of wind turbines participation at nominal parameters The robustness of the proposed DMPC scheme is also verified by two cases. The performance and the implementation of the proposed DMPC are compared with other two types of typical LFC scheme.

The centralized MPC and decentralized MPC controller are designed for four area interconnected power system, respectively. The four-area interconnected power system can be described as

$$x(k+1) = Ax(k) + Bu(k) + Fd(k)$$
$$y(k+1) = Cx(k) \tag{24}$$

where

$$A = \begin{bmatrix} A_{11} & A_{12} & A_{13} & A_{14} \\ A_{21} & A_{22} & A_{23} & A_{24} \\ A_{31} & A_{32} & A_{33} & A_{34} \\ A_{41} & A_{42} & A_{43} & A_{44} \end{bmatrix}$$

$$B = \begin{bmatrix} B_{11} & B_{12} & B_{13} & B_{14} \\ B_{21} & B_{22} & B_{23} & B_{24} \\ B_{31} & B_{32} & B_{33} & B_{34} \\ B_{41} & B_{42} & B_{43} & B_{44} \end{bmatrix}$$

$$C = \begin{bmatrix} C_{11} & 0 & 0 & 0 \\ 0 & C_{22} & 0 & 0 \\ 0 & 0 & C_{33} & 0 \\ 0 & 0 & 0 & C_{44} \end{bmatrix}$$

$$F = \begin{bmatrix} F_{11} & 0 & 0 & 0 \\ 0 & F_{22} & 0 & 0 \\ 0 & 0 & F_{33} & 0 \\ 0 & 0 & 0 & F_{44} \end{bmatrix}$$

$$x = \begin{bmatrix} x_1^T & x_2^T & x_3^T & x_4^T \end{bmatrix}^T$$

$$u = \begin{bmatrix} u_1^T & u_2^T & u_3^T & u_4^T \end{bmatrix}^T$$

$$y = \begin{bmatrix} y_1^T & y_2^T & y_3^T & y_4^T \end{bmatrix}^T$$

$$d = \begin{bmatrix} d_1^T & d_2^T & d_3^T & d_4^T \end{bmatrix}^T$$

with constraints (20) and (23) for each control area. In centralized MPC framework, the MPC for the overall system (23) solves the following optimization problem:

$$\min_{u(k+n|k)} J(k) \tag{25}$$

$$J(k) = \sum_{n=0}^{N_P} [x^T(k+n|k)Qx(k+n|k) + u^T(k+n|k)Ru(k+n|k)] \tag{26}$$

subject to (20) and (23).

The weighting matrices $Q$ and $R$ in the objective function (26) are chosen as $R = \mathrm{diag}\,\{1,1,1,1\}$.

$$Q = \mathrm{diag}\{1000, 0, 0, 1000, 1000, 0, 0, 1000,$$
$$1000, 0, 0, 1000, 1000, 0, 0, 1000\}.$$

In the decentralized modeling framework, it is assumed that the interaction between the control areas is negligible. Subsequently, the decentralized model for each control area is

$$x_i(k+1) = A_{ii}x_i(k) + B_{ii}u_i(k) + F_{ii}d_i(k)$$
$$y_i(k+1) = C_{ii}x_i(k) \tag{27}$$

with the system matrices are same as the distributed model, as shown in Section II and the constraints (20) and (23) for each control area. In decentralized MPC framework, each control area based MPC solves the following optimization problem:

$$\min_{u_i(k+n|k)} J_i(k) \tag{28}$$

$$J_i(k) = \sum_{n=0}^{N} [x_i^T k + n|k)Q_i x_i(k + n|k)$$
$$+ u_i^T(k + n|k)R_i u_i(k + n|k)] \qquad (29)$$

subject to (20) and (23).

The weighting matrices $Q_i$ and $R_i$ in the objective function (29) are chosen as $R_1 = R_2 = R_3 = R_4 = 1$.

$$Q_1 = Q_2 = Q_3 = Q_4 = \text{diag}\{1000, 0, 0, 1000\}.$$

Choose the prediction horizon of the centralized MPC, decentralized MPC and distributed MPC to be $N = 15$, the control horizon to be $N_c = 10$, the sample time $T_s = 0.1$, $\lambda = 0.1$. In addition, the Area 1 includes an aggregated wind turbine model which consists of 40 wind turbine units of 2 MW rated DFIGs while the capacity of thermal plant is 600 MW. The wind turbine parameters and operating points are indicated in Table II [20]. The parameters used in the simulation are listed in Table III.

TABLE II
OPERATING POINT AND PARAMETERS FOR THE WIND TURBINE

| Parameters |
| --- |
| Operating point: 80 MW,  wind speed: 17 m/s |
| $R_r = 0.00552$ pu,  $R_s = 0.00491$ pu,  $w_{opt} = 1.15$ m/s |
| $L_m = 3.9654$ pu,  $L_{rr} = 0.1$ pu,  $L_{ss} = 0.09273$ pu |
| $H_t = 4.5$ pu,  $w_s = 1.17$ m/s |

TABLE III
PARAMETERS FOR THE THERMAL POWER PLANTS

| Parameters |
| --- |
| $K_{P1} = 120$ Hz/p.u.MW,  $K_{P2} = 115$ Hz/p.u.MW |
| $K_{P3} = 80$ Hz/p.u.MW,  $K_{P4} = 75$ Hz/p.u.MW |
| $T_{P1} = 20$ s,  $T_{P2} = 20$ s,  $T_{P3} = 13$ s,  $T_{P4} = 15$ s |
| $R_1 = 2.4$ Hz/p.u.MW,  $R_2 = 2.5$ Hz/p.u.MW |
| $R_3 = 3.3$ Hz/p.u.MW,  $R_4 = 3$ Hz/p.u.MW |
| $K_{B1} = 0.425$ p.u.MW/Hz,  $K_{B2} = 0.409$ p.u.MW/Hz |
| $K_{B3} = 0.316$ p.u.MW/Hz,  $K_{B4} = 0.347$ p.u.MW/Hz |
| $T_{G1} = 0.08$ s,  $T_{G2} = 0.1$ s,  $T_{G3} = 0.08$ s,  $T_{G4} = 0.2$ s |
| $T_{T1} = T_{T4} = 0.3$ s,  $T_{r1} = T_{r4} = 10$ s,  $T_{R2} = 0.6$ s,  $T_{R3} = 0.513$ s |
| $K_{Sij} = -K_{Sij} = 0.545$ p.u.MW |

### A. Case 1: Response to Step Load Change Without Wind Turbines Participation

Wind turbine is present but it does not provide any power support in the event of grid frequency deviation. An event is simulated in which a system shown in Fig. 1 is subjected to step load disturbances as given in (29) at $t = 10$ s.

$$\Delta P_{d1} = \Delta P_{d3} = 0.1. \qquad (30)$$

The relative performance of distributed MPC, centralized-MPC and decentralized MPC rejecting the load disturbance in each area are shown in Fig. 5 as solid, dotted and dashed lines respectively. From the results, distributed MPC controller in each area regulates generated power to match the load fluctuations effectively. The performance of the centralized MPC

is almost identical to the proposed DMPC controllers. This is because the complete state information for all generators is known globally, the optimal solutions can be solved accurately with the valve position constraints and GRCs. However, the frequency deviation is damped to zero with big oscillations by decentralized MPC controllers due to the connections between the control areas are fully negligible.
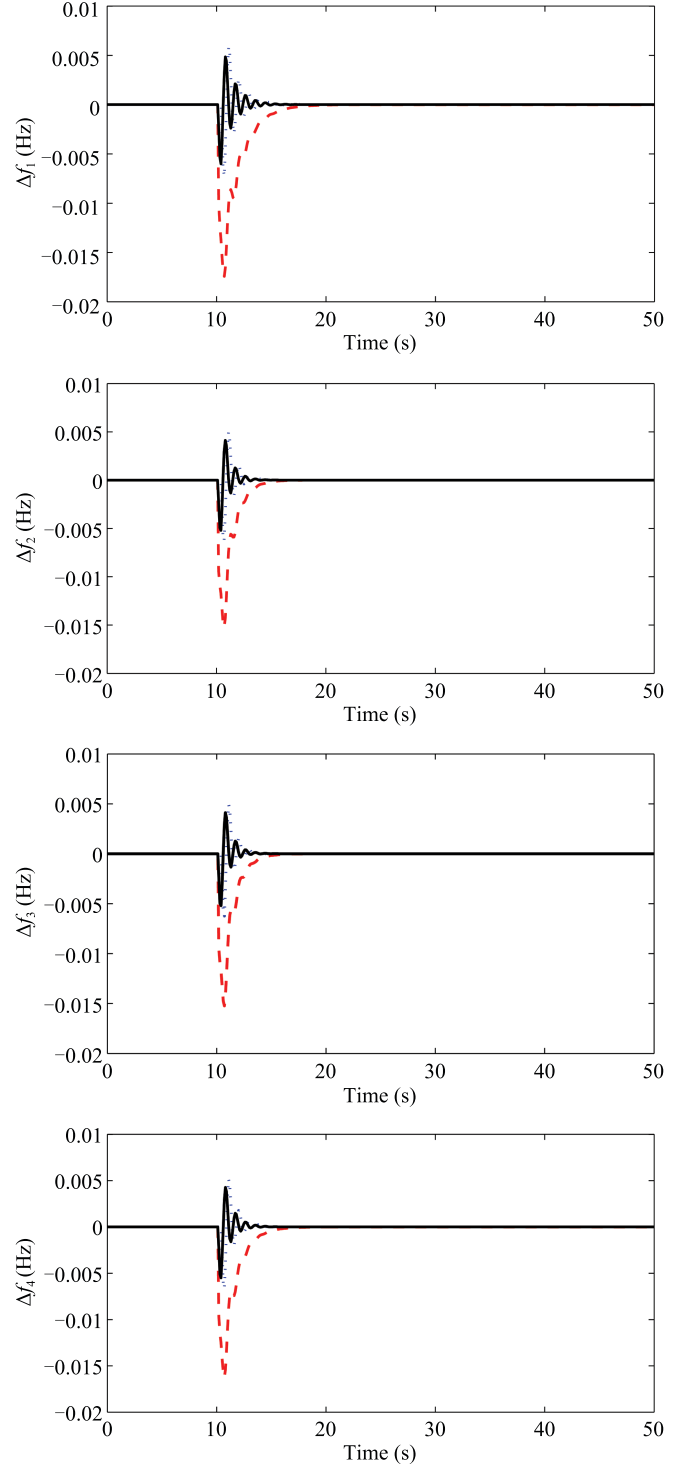


Fig. 5.   Response of frequency deviation to step load disturbance in Case 1: distributed MPC (solid line), centralized MPC (dotted line) and decentralized MPC (dashed line).

The control costs defined by [19] for different strategies are listed in Table IV. It is obviously seen that the DMPC controller needs nearly as much CPU time as decentralized MPC controller and significantly less CPU time than centralized MPC controllers. The proposed DMPC algorithm has significant computational advantages when compared to centralized MPC while achieving the best performance.

TABLE IV
COST OF THE DIFFERENT STRATEGIES

| Strategy | Cost [20] |
| --- | --- |
| Centralized MPC | 0.10 |
| Decentralized MPC | 0.083 |
| Distributed MPC | 0.078 |

### B. Case 2: Response to Step Load Change With Wind Turbines Participation

Wind turbine is present and it will provide active power support in the event of grid frequency deviation. During the wind farm operation, it is assumed that the mean wind speed of a certain period can be estimated. The 1-min turbulent wind sequence with a mean value of 17 m/s is adopted in the simulation [24], which covers the range between 15 and 20 m/s. An event is simulated in which a system shown in Fig.1 is subjected to step load disturbances as shown in (30) at $t = 10$ s.

In Fig. 6 and Fig. 7, the behavior for the frequency is presented for Case 1 where the wind turbines are participating in load frequency control. The results from top to the bottom in Fig. 6 are: the frequency deviations for Area 1 to Area 4, and in Fig. 7 are: six tie-lines power change. In simulation, it is obvious that both the DMPC and the centralized MPC converge rapidly and drive the local frequency changes and tie-line power deviation to zero. The wind turbines that have participated in the interconnected power system do not affect the performance of the power system under distributed MPC and centralized MPC while satisfying all the physical constraints, e.g., the GRC, the limit of the wind speed and load step change constraints. However, with decentralized MPC, the rapid convergence cannot be guaranteed in the presence of wind turbines in Area 1. This is because the GRCs and load step change constraints cannot be guaranteed in the presence of random wind power output. This confirms the performance advantage of the proposed distributed model predictive control algorithm.

Fig. 8 shows the dynamic response of active power deviation $\Delta P_e$ and rotor speed $\omega_g$ of wind turbine while participating for the load frequency control. When the control is activated, the frequency deviation becomes zero which consequently eliminated the additional active power deviation $\Delta P_e$ and wind turbine is driven to operate again at the optimal rotor speed $\omega_g$. It may be noted here that an increase in power step on top of the converter further reduces the rotor speed, thereby transferring more kinetic power to reduce the frequency dip. As shown in this figure, the distributed MPC in the presence of wind turbine has desirable performance in comparison to centralized MPC and decentralized MPC. Fig. 9 shows the generating outputs of traditional plants.
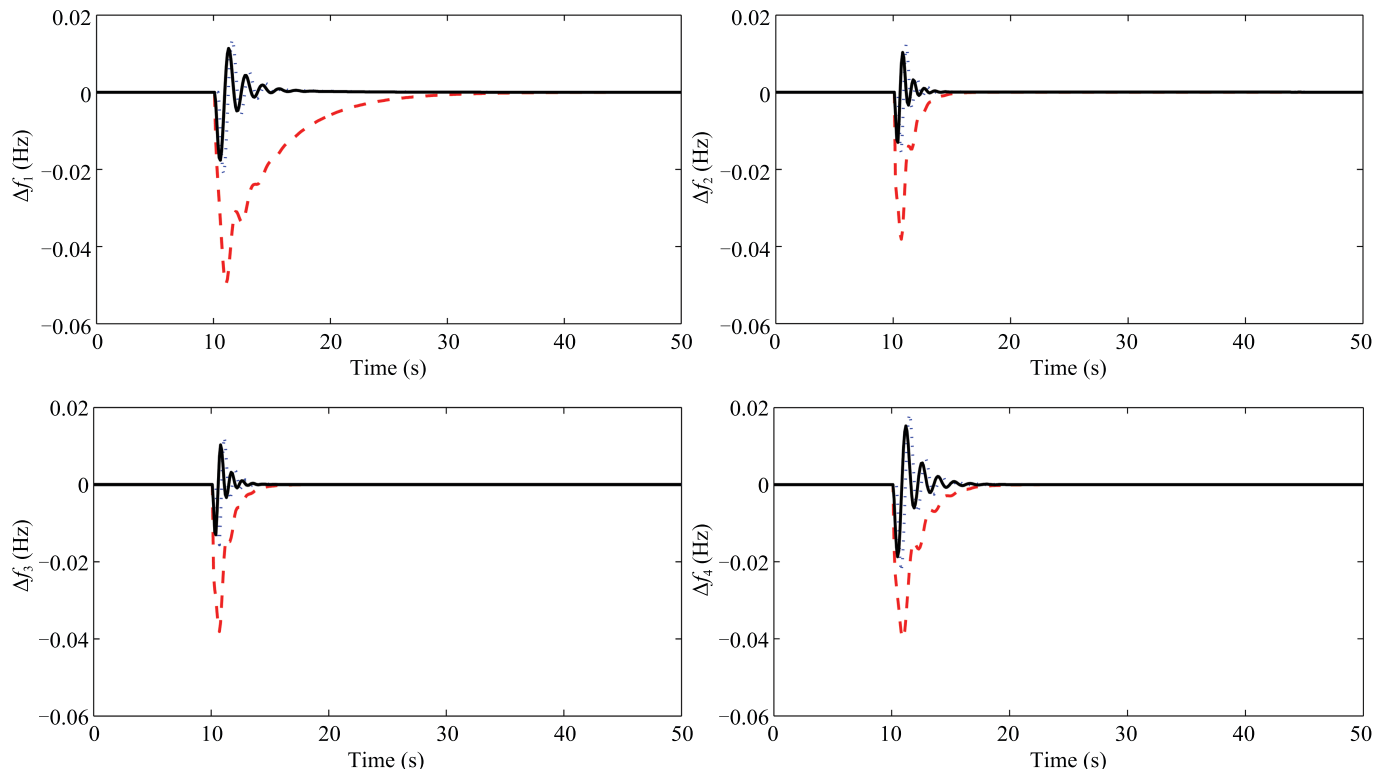


Fig. 6.    Response of frequency deviation to step load disturbance 2: distributed MPC (solid line), centralized MPC (dotted line) and decentralized MPC (dashed line).
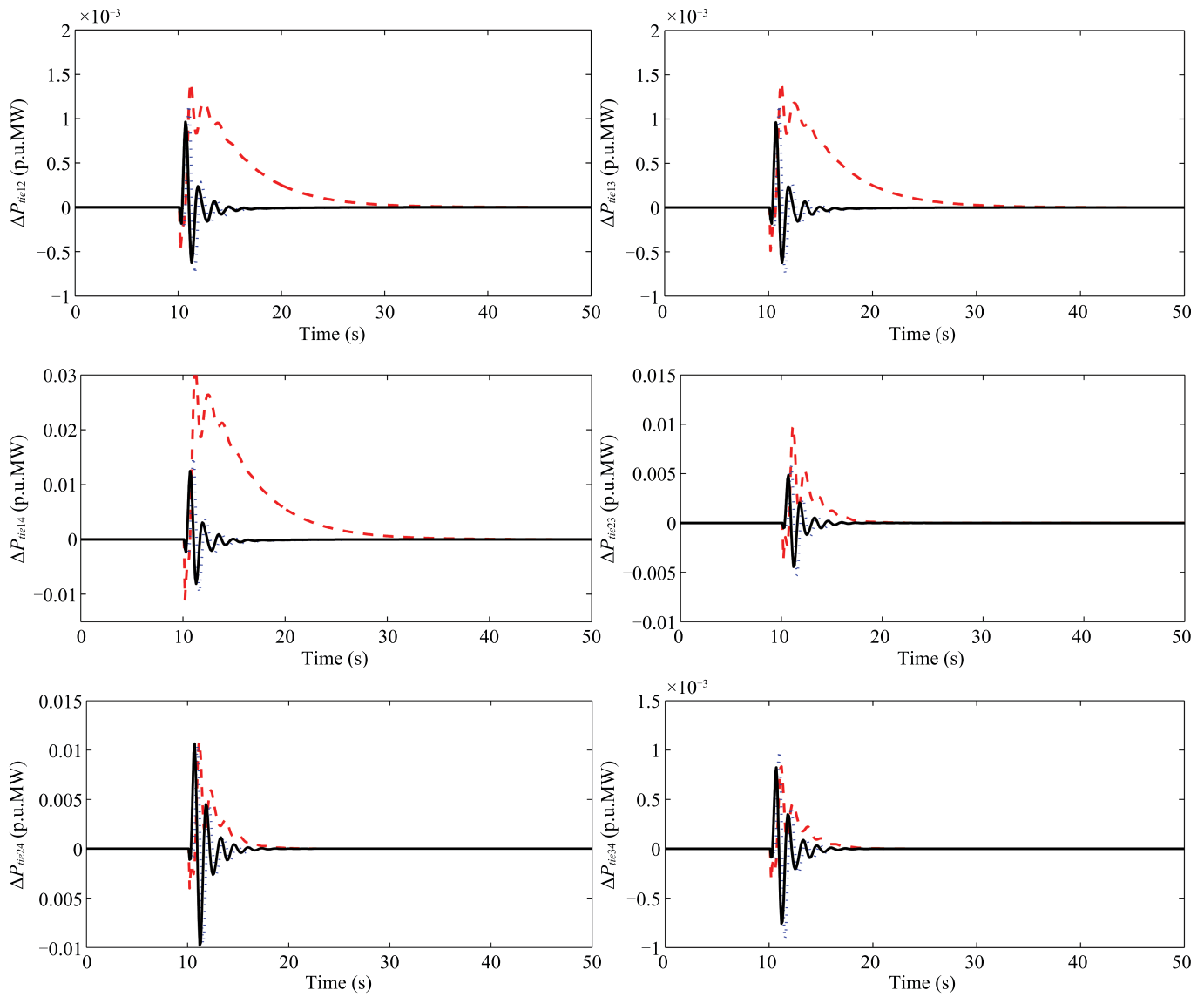
Fig. 7. Response of tie-line active power deviation in Case 2: distributed MPC (solid line), centralized MPC (dotted line) and decentralized MPC (dashed line).
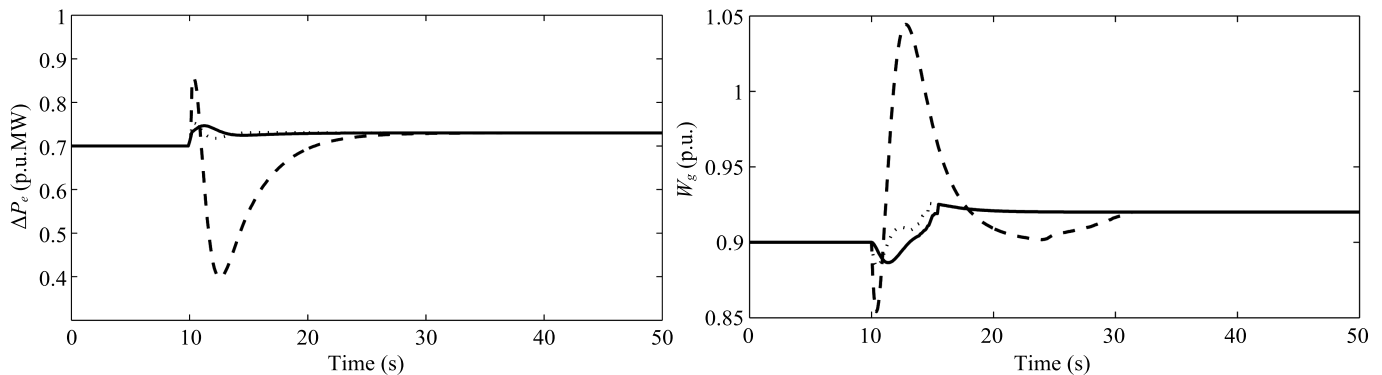


Fig. 8. Wind turbine response of electrical power, rotor speed in Case 2: distributed MPC (solid line), centralized MPC (dotted line) and decentralized MPC (dashed line).
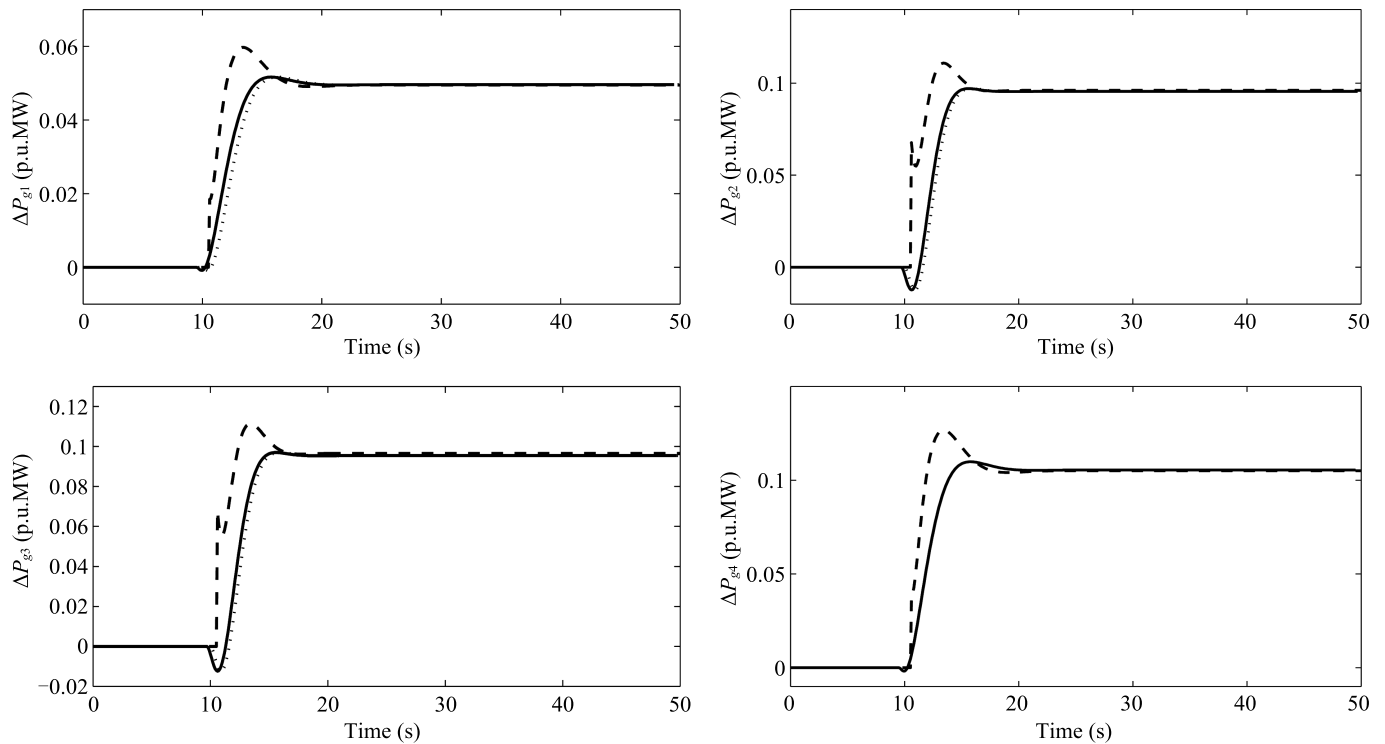
Fig. 9.    Response of generated power deviation in Case 2: distributed MPC (solid line), centralized MPC (dotted line) and decentralized MPC (dashed line).

## V. CONCLUSION

This paper studies the merging of wind turbines in the four-area interconnected power system load frequency controlled by the distributed model predictive control with input and state constraints. The four-area interconnected power system composed of wind turbine and thermal plant, each control area has a local MPC controller, in which the four controllers coordinate with each other by exchanging their information. Digital simulations have been carried out in order to validate the effectiveness of the proposed DMPC scheme. Comparisons of response to step load change, computational burden and robustness have been made between DMPC, centralized MPC and decentralized MPC. The results confirm the superiority of the proposed DMPC technique.

## REFERENCES

[1] H. Shayeghi, H. A. Shayanfar, and A. Jalili, "Load frequency control strategies: a state-of-the-art survey for the researcher," *Energ. Convers. Manage.*, vol. 50, no. 2, pp. 344−353, Feb. 2009.

[2] H. Bevrani, F. Daneshfar, and P. R. Daneshmand, "Intelligent power system frequency regulations concerning the integration of wind power units," in *Wind Power Systems: Applications of Computational Intelligence*, L. F. Wang, C. Singh, and A. Kusiak, Eds. Berlin Heidelberg: Springer, 2010, pp. 407−437.

[3] Y. C. Xue and N. L. Tai, "Review of contribution to frequency control through variable speed wind turbine," *Renew. Energ.*, vol. 36, no. 6, pp. 1671−1677, Jun. 2011.

[4] Global Wind Energy Council, *Global Wind Report on Annual Market*. Germany: Global Wind Energy Council, 2014.

[5] Y. Z. Sun, Z. S. Zhang, G. J. Li, and J. Lin, "Review on frequency control of power systems with wind power penetration," in *Proc. 2010 Int. Conf. Power System Technology*, Hangzhou, China, 2010, pp. 1−8.

[6] S. K. Pandey, S. R. Mohanty, and N. Kishor, "A literature survey on load-frequency control for conventional and distribution generation power systems," *Renew. Sustain. Energ. Rev.*, vol. 25, pp. 318−334, Sep. 2013.

[7] F. Díaz-González, M. Hau, A. Sumper, and O. Gomis-Bellmunt, "Participation of wind power plants in system frequency control: review of grid code requirements and control methods," *Renew. Sustain. Energ. Rev.*, vol. 34, pp. 551−564, Jun. 2014.

[8] L. R. Chang-Chie, C. C. Sun, and Y. J. Yeh, "Modeling of wind farm participation in AGC," *IEEE Trans. Power Syst.*, vol. 29, no. 3, pp. 1204−1211, May 2014.

[9] H. Bevrani and P. R. Daneshmand, "Fuzzy logic-based load-frequency control concerning high penetration of wind turbines," *IEEE Syst. J.*, vol. 6, no. 1, pp. 173−180, Mar. 2012.

[10] M. H. Variani and K. Tomsovic, "Distributed automatic generation control using flatness-based approach for high penetration of wind generation," *IEEE Trans. Power Syst.*, vol. 28, no. 3, pp. 3002−3009, Aug. 2013.

[11] X. J. Liu, P. Guan, and C. W. Chan, "Nonlinear multivariable power plant coordinate control by constrained predictive scheme," *IEEE Trans. Contr. Syst. Technol.*, vol. 18, no. 5, pp. 1116−1125, Sep. 2010.

[12] X. J. Liu and C. W. Chan, "Neuro-fuzzy generalized predictive control of boiler steam temperature," *IEEE Trans. Energ. Conserv.*, vol. 21, no. 4, pp. 900−908, Dec. 2006.

[13] X. J. Liu and X. B. Kong, "Nonlinear fuzzy model predictive iterative learning control for drum-type boiler-turbine system," *J. Process Contr.*, vol. 23, no. 8, pp. 1023−1040, Sep. 2013.

[14] X. J. Liu, X. B. Kong, and X. Z. Deng, "Power system model predictive load frequency control," in *Proc. 2012 American Control Conf.*, Montreal, QC, 2012, pp. 6602−6607.

[15] T. H. Mohamed, J. Morel, H. Bevrani, and T. Hiyama, "Model predictive

based load frequency control-design concerning wind turbines," *Int. J. Electric. Power Energ. Syst.*, vol. 43, no. 1, pp. 859−867, Dec. 2012.

[16] T. H. Mohamed, H. Bevrani, A. A. Hassan, and T. Hiyama, "Decentralized model predictive based load frequency control in an interconnected power system," *Energ. Convers. Manage.*, vol. 52, no. 2, pp. 1208−1214, Feb. 2011.

[17] Y. Zheng, S. Y. Li, and H. Qiu, "Networked coordination-based distributed model predictive control for large-scale system," *IEEE Trans. Contr. Syst. Technol.*, vol. 21, no. 3, pp. 991−998, May 2013.

[18] E. Camponogara and H. F. Scherer, "Distributed optimization for model predictive control of linear dynamic networks with control-input and output constraints," *IEEE Trans. Autom. Sci. Eng.*, vol. 8, no. 1, pp. 233−242, Jan. 2011.

[19] A. N. Venkat, I. A. Hiskens, J. B. Rawlings, and S. J. Wright, "Distributed MPC strategies with application to power system automatic generation control," *IEEE Trans. Contr. Syst. Technol.*, vol. 16, no. 6, pp. 1192−1206, Nov. 2008.

[20] J. Morel, H. Bevrani, T. Ishii, and T. Hiyama, "A robust control approach for primary frequency regulation through variable speed wind turbines," *IEEJ Trans. Power Energ.*, vol. 130, no. 11, pp. 1002−1009, Nov. 2010.

[21] M. Yigit, V. C. Gungor, G. Tuna, M. Rangoussi, and E. Fadel, "Power line communication technologies for smart grid applications: a review of advances and challenges," *Comput. Networks*, vol. 70, pp. 366−383, Sep. 2014.

[22] A. J. Wood and B. F. Wollenberg, *Power Generation Operation and Control*. New York: Wiley, 1996.

[23] W. B. Dunbar and R. M. Murray, "Distributed receding horizon control for multi-vehicle formation stabilization," *Automatica*, vol. 42, no. 4, pp. 549−58, Apr. 2006.

[24] V. Spudić, M. Jelavić, and M. Baotić, "Wind turbine power references in coordinated control of wind farms," *Automatika-J. Contr. Measure. Electron. Comput. Commun.*, vol. 52, no. 2, pp. 82−94, Jul. 2011.
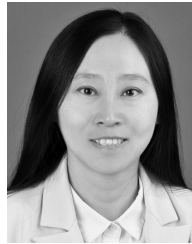
**Yi Zhang** received her master degree from North China Electric Power University, China, in 2008. She is currently a Ph.D. candidate in automatic control at North China Electric Power University and she is a lecturer at the North China University of Science and Technology. Her research interests include modeling, distributed model predictive control and robust control and its application in load frequency control of power system. Corresponding author of this paper.



**Xiangjie Liu** received his Ph.D. degree in electrical and electronic engineering from the Research Center of Automation, Northeastern University, China, in 1997. He subsequently held a postdoctoral position with the China Electric Power Research Institute (CEPRI), Beijing, China, until 1999. He has been an associate professor at CEPRI since 1999. He was a research associate with the University of Hong Kong, and a professor with National University of Mexico. He is currently a professor with the Department of Automation, North China Electric Power University, Beijing, China. His current research interests include fuzzy control, neural networks, model predictive control with its application in industrial processes.



**Bin Qu** received his B.S. degree in agricultural electrification automation in 1998, his master degree in agricultural mechanization engineering at Mechanical and Electrical College, Agricultural University of Hebei, Baoding, China in 2003. He is currently a Ph.D. candidate at Hebei University of Technology and he is an associate-professor at North China University of Science and Technology. His research interests include modeling, distributed model predictive control and robust control and with its application.